

NOTES AND CORRESPONDENCE

Note on “Predictability of Northeast Brazil Rainfall and Real-Time Forecast Skill, 1987–98”

IRACEMA F. A. CAVALCANTI

Center of Weather Forecast and Climate Studies, CPTEC/INPE, Sao Paulo, Brazil

CHRIS K. FOLLAND AND ANDREW W. COLMAN

Hadley Centre for Climate Prediction and Research, Met Office, Bracknell, Berkshire, United Kingdom

5 November 2001 and 18 December 2001

1. Introduction

We comment on speculations in Folland et al. (2001, hereafter FCRD) about atmospheric and oceanic influences on northeast Brazil (NEB) rainfall in the austral winter dry season. FCRD was mainly concerned with the NEB wet season and its predictability. However, the paper also touched upon the dry season, particularly June and July, when there is sometimes appreciable rainfall. Figure 3d of FCRD showed correlations of the worldwide Global Sea Ice and Sea Surface Temperature version 3 (GISST3) dataset with NEB rainfall, showing areas of fairly strong correlation with Atlantic SST, particularly in the tropical South Atlantic on the South American side of that ocean. FCRD speculated that the high correlation of NEB rainfall with SST in the tropical Atlantic Ocean in June–July might be associated with a displacement of the South Atlantic convergence zone (SACZ) northward. We want to correct this hypothesis, and indicate possible links between June–July NEB rainfall and tropical South Atlantic SST.

Analyses of the tropical and subtropical precipitation zones in the Southern Hemisphere have been performed by Kodama (1992, 1993), including the SACZ. Other studies that show influences of the SACZ were reported in Kousky (1988), Liebmann et al. (1999), and Nogues-Paegle and Mo (1997). The SACZ is a band of cloudiness and convective activity oriented northwest–southeast (NW–SE) over eastern South America extending

into the tropical to subtropical South Atlantic. It is seen from the end of austral spring (November) up to the beginning of austral autumn (March), being more frequent in the summer months. The SACZ can be detected in both monthly mean precipitation and outgoing long-wave radiation (OLR) fields. From about April to October the higher values of precipitation and low values of OLR are displaced northwestward. The SACZ ceases to exist in the austral winter half year. At the same time, there is another band of precipitation over southern Brazil, associated with frequent passages of frontal systems. The SACZ can influence NEB rainfall, but only in the austral summer when it can be displaced northward and affects southern NEB (Chaves and Cavalcanti 2001).

2. Further analyses of the influence of SST on tropical South American precipitation

Figure 1 shows the seasonal climatology of precipitation over South America from the Climate Prediction Center Merged Analysis of Precipitation (CMAP) dataset (Xie and Arkin 1997). There is rainfall over the eastern coast of NEB in June–August but little in September–November (see Fig. 1 of FCRB for the location of NEB rainfall as considered here). In the austral summer [December–January–February (DJF)], the band of NW–SE-orientated precipitation extending from the Amazonia region to the Atlantic Ocean represents the effect of the SACZ. In MAM and JJA the higher values of precipitation and low values of OLR are displaced northwestward, and in SON they start to extend again southeastward. The band of precipitation to the south that exists from MAM to SON, including the winter JJA season, is also clearly visible. It extends much more

Corresponding author address: Dr. Iracema F. A. Cavalcanti, Center of Weather Forecast and Climate Studies, CPTEC/INPE, Rodovia Presidente Dutra, Km 40, Cachoeira Paulista, S.P., CEP 126 30-000, Brazil.
E-mail: Iracema@cptec.inpe.br

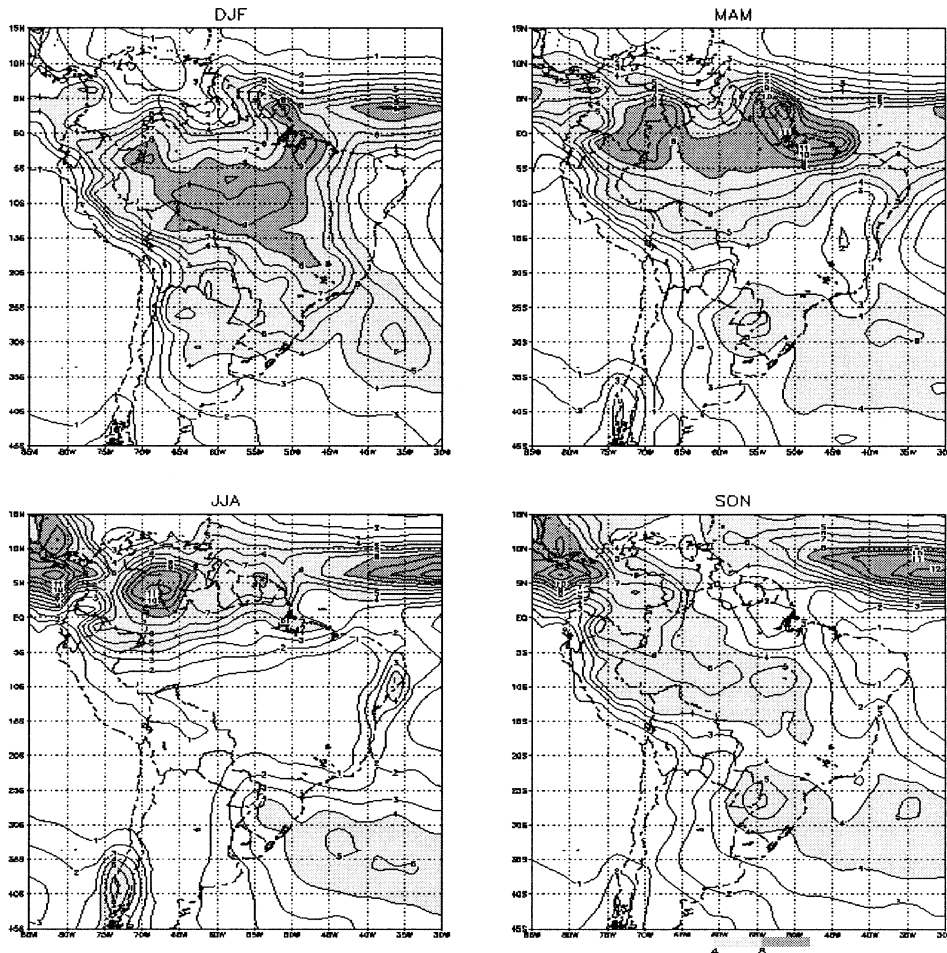


FIG. 1. Seasonal climatology of precipitation (mm day^{-1}) from CMAP data (Xie and Arkin 1997) over South America to 50°S for the period 1979–98. Contour interval is 1 mm day^{-1} .

east–west in these seasons than does the more northerly displaced SACZ in austral summer.

We now investigate the influence of SST in the tropical South Atlantic, averaged over June and July, on atmospheric circulation and precipitation over tropical South America for the same months. To provide an SST index, we use the average SST anomaly in the region $10^{\circ}\text{--}20^{\circ}\text{S}$, $35^{\circ}\text{--}22.5^{\circ}\text{W}$ where the strongest relationships in Fig. 3d of FCRD were found. Extension of this SST area eastward to 10°W gives similar but weaker results to those described below. The atmospheric data, including precipitation, is taken from the National Centers for Environmental Prediction–National Center for Atmospheric Research (NCEP–NCAR) reanalysis (Kalnay et al. 1996) for 1958–98. Most of our analyses are based on differences between mean atmospheric anomalies in the 10 warmest and 10 coolest years in the above SST region over the period 1958–98, applying the GISST3 dataset used in FCRD.

Figure 2 shows the differences in precipitation between the warm and cold years. There is a long band

of significant differences stretching along the northeast coast of South America from north of the equator to just south of the SST region. Differences are particularly large over the western part of NEB, but are significant everywhere over that region and represent a major modulation of rainfall in this rather dry season compared to the rainfall climatology (Fig. 1). Not surprisingly, the correlation between SST and precipitation (not shown) is highly significant and positive, and exceeds 0.4 over many NEB subregions (areas $2.5^{\circ} \text{ lat} \times 3.75^{\circ} \text{ lon}$), as well as over the coastal region to the south of Cape San Roque, Rio Grande do Norte. Precipitation over the western half of the SST region itself is also significantly positively correlated with SST. This precipitation band over the Atlantic Ocean may be related to the influence of frontal systems on NEB precipitation as mentioned in Kousky (1979). Significant correlations are surprisingly extensive with a large band of negative correlations over the tropical North Atlantic Ocean and Caribbean Sea that deserve more attention.

Further insight is given by Figs. 3a and 3b. Figure

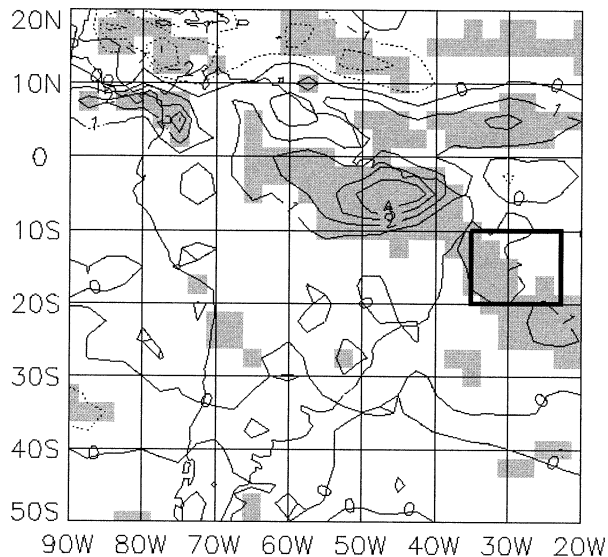


FIG. 2. The difference in precipitation (mm day^{-1}) averaged for Jun and Jul over South America to 50°S between the 10 yr of warmest SST in the region $10^{\circ}\text{--}20^{\circ}\text{S}$, $35^{\circ}\text{--}22.5^{\circ}\text{W}$ and the 10 coldest yr, 1958–98 (boxed in black). Contour interval is 1 mm day^{-1} . Differences statistically significant at the 5% confidence level given by a local t test are shaded.

3a shows the difference in the convergence of near-surface (10 m) winds between years with warm and cold SST. A highly significant difference is seen over NEB and part of the coast to the southeast. Over the drier parts of northern NEB this is sufficient to change the net mean absolute divergence (cold SST) to absolute convergence (warm SST). Figure 3b shows the difference in near-surface vector winds. The main feature is a southward anomalous flow from the tropical Atlantic from 10°N southward into NEB in warm SST years that then extends south to the SST region itself. Significant (thick) arrows are those where differences in either u or v components of the flow are significant at the 5% level. This behavior of the winds is quite like that shown by the difference in u and v between wet and dry years in the main rainfall season (Fig. 11 of FCRD). However, the detailed mechanisms must be somewhat different as the ITCZ is farther north in austral winter.

3. Conclusions

Much of the earlier work in austral winter on variations in rainfall in this general region has been done for the coastal area southeast of the NEB region considered here (e.g., Kousky 1979, 1980; Rao et al. 1993). These authors give physical explanations about the mechanisms of precipitation over this region in the winter season. This region is seaward of a near-coastal mountain range stretching south from near Cape San Roque, and has a wetter austral winter climate. Clearly it is affected by the SST changes shown here too. Rain-

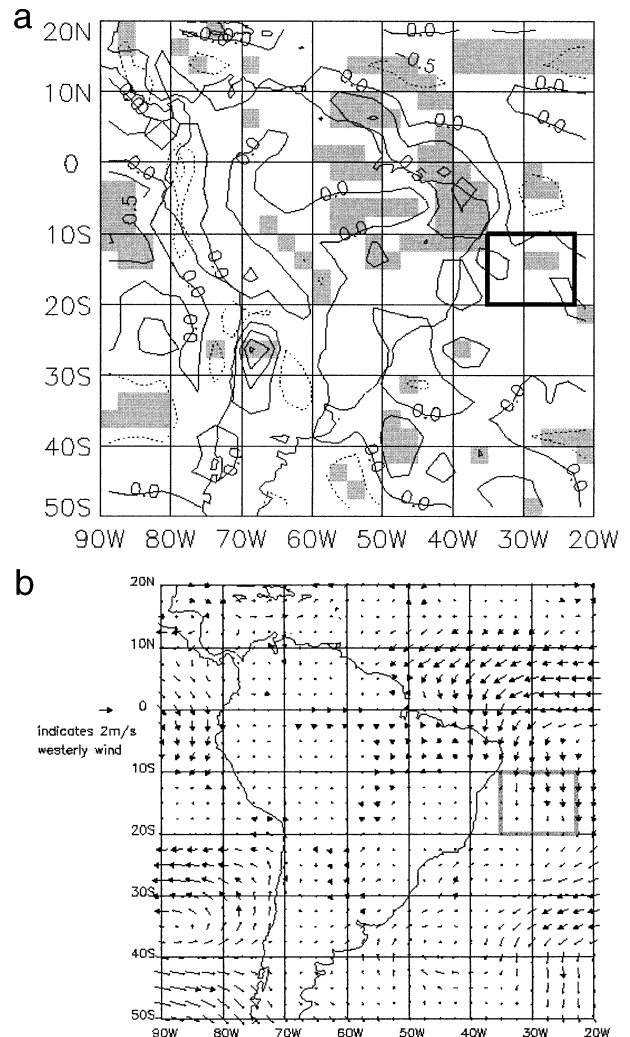


FIG. 3. (a) As in Fig. 2, difference in the convergence of near-surface winds between the average of the 10 warmest SST yr and the 10 coldest SST yr. Positive values represent increased convergence. Contour interval is 0.5 m s^{-1} . SST region is boxed in black. (b) Difference in near-surface winds (m s^{-1}) between average of the 10 warmest SST yr and the 10 coldest SST yr. The shaded square shows the SST region. Arrow lengths are proportional to wind speed. Thick arrows show where difference in westerly or northerly wind component is 5% significant according to t test.

fall in austral winter has been related to convection associated with eastern disturbances that can be seen in satellite infrared images. Yamazaki and Rao (1977) suggested that westward-propagating cloud systems were responsible for the May–July monthly precipitation maximum along the eastern coast of NEB. So it is possible that the large-scale flow and convergence changes shown here both influence, and result from, such synoptic-scale westward-propagating waves over the NEB region. Perhaps these waves are more vigorous over NEB in warm SST years than in cold ones. Daily surface and satellite data should be used to investigate this idea.

However, it does not seem likely from these results that the austral winter east–west extratropical rainfall band well to the south of NEB plays an appreciable role.

REFERENCES

- Chaves, R. R., and I. F. A. Cavalcanti, 2001: Atmospheric features associated with rainfall variability over southern Northeast Brazil. *Mon. Wea. Rev.*, **129**, 2614–2626.
- Folland, C. K., A. W. Colman, D. P. Rowell, and M. K. Davey, 2001: Predictability of Northeast Brazil rainfall and real-time forecast skill, 1987–98. *J. Climate*, **14**, 1937–1958.
- Kalnay, E., and Coauthors, 1996: The NCEP/NCAR 40-Year Reanalysis Project. *Bull. Amer. Meteor. Soc.*, **77**, 437–471.
- Kodama, Y., 1992: Large-scale common features of subtropical precipitation zones (the Baiu frontal zone, the SPCZ, and the SACZ). Part I: Characteristics of the subtropical frontal zones. *J. Meteor. Soc. Japan*, **70**, 813–836.
- , 1993: Large-scale common features of subtropical precipitation zones (the Baiu frontal zone, the SPCZ, and the SACZ). Part II: Conditions of the circulation for generating the STCZs. *J. Meteor. Soc. Japan*, **71**, 581–610.
- Kousky, V. E., 1979: Frontal influences on Northeast Brazil. *Mon. Wea. Rev.*, **107**, 1140–1153.
- , 1980: Diurnal rainfall variation in Northeast Brazil. *Mon. Wea. Rev.*, **108**, 488–498.
- , 1988: Pentad outgoing longwave radiation climatology for the South American sector. *Rev. Bras. Meteor.*, **3**, 217–231.
- Liebmann, B., G. N. Kiladis, J. A. Marengo, T. Ambrizzi, and J. D. Glick, 1999: Submonthly convective variability over South America and the South Atlantic convergence zone. *J. Climate*, **12**, 1877–1891.
- Nogues-Paegle, J., and K. C. Mo, 1997: Alternating wet and dry conditions over South America during summer. *Mon. Wea. Rev.*, **125**, 279–291.
- Rao, V. B., M. L. C. Lima, and S. Franchito, 1993: Seasonal and interannual variations of rainfall over eastern northeast Brazil. *J. Climate*, **6**, 1754–1763.
- Xie, P., and P. A. Arkin, 1997: Global precipitation: A 17-year monthly analysis based on gauge observations, satellite estimates, and numerical model outputs. *Bull. Amer. Meteor. Soc.*, **78**, 2539–2558.
- Yamazaki, Y., and V. B. Rao, 1977: Tropical cloudiness over the South Atlantic Ocean. *J. Meteor. Soc. Japan*, **55**, 205–207.